The origin and diversification of pteropods predate past perturbations in the Earth's carbon cycle

Katja T.C.A. Peijnenburg[1,2,*], Arie W. Janssen[1], Deborah Wall-Palmer[1], Erica Goetze[3], Amy Maas[6], Jonathan A. Todd[4], Ferdinand Marlétaz[5,*]

[*] Corresponding authors: Katja T.C.A. Peijnenburg, Ferdinand Marlétaz

[1] Marine Biodiversity, Naturalis Biodiversity Center, P.O. Box 9517, 2300 RA Leiden, The Netherlands

[2] Department Freshwater and Marine Ecology, Institute for Biodiversity and Ecosystem Dynamics, University of Amsterdam, P.O. Box 94248, 1090 GE Amsterdam, The Netherlands

[3] Department of Oceanography, School of Ocean and Earth Science and Technology, University of Hawai'i, Honolulu, United States of America

[4] Department of Earth Sciences, Natural History Museum London, SW7 5BD, United Kingdom

[5] Molecular Genetics Unit, Okinawa Institute of Science and Technology, Onna-son, Japan

[6] Bermuda Institute of Ocean Sciences, St. Georges GE01, Bermuda

Summary

Pteropods are a group of planktonic gastropods that are widely regarded as biological indicators for assessing the impacts of ocean acidification (OA). Their thin aragonitic shells are highly sensitive to acute changes in ocean chemistry. However, to gain insight into their potential to adapt to current climate change, we need to accurately reconstruct their evolutionary history and assess their responses to past changes in Earth's carbon cycle. Here, we resolve the phylogeny and timing of pteropod evolution with a phylogenomic dataset incorporating 21 new species and new fossil evidence. In agreement with traditional taxonomy, we recovered the first molecular support for a division between sea butterflies (Thecosomata: mucus-web feeders) and sea angels (Gymnosomata: active predators). Molecular dating demonstrated that these two lineages diverged in the early Cretaceous, and that all main pteropod clades, including shelled, partially-shelled and unshelled groups, diverged in the mid to late Cretaceous. Hence, these clades originated prior to and subsequently survived major global change

events, including the Paleocene Eocene Thermal Maximum (PETM), which is the closest analogue to modern-day ocean acidification and warming. Our findings indicate that aragonitic calcifiers have been resilient to extreme perturbations in the Earth's carbon cycle over evolutionary timescales.

Introduction

Pteropods are marine gastropods that spend their entire life in the open water column. A remarkable example of adaptation to pelagic life, these mesmerizing animals have thin shells and a snail foot transformed into two wing-like structures that enable them to 'fly' through the water column (Fig. 1). Pteropods are a common component of marine zooplankton assemblages worldwide, where they serve important trophic roles in pelagic food webs, and are major contributors to carbon and carbonate fluxes in the open ocean (Berner and Honjo 1981; Hunt et al. 2008; Bednaršek et al. 2012a; Manno et al. 2018; Buitenhuis et al. 2019).

Shelled pteropods have been a particular focus for global change research because they make their shells of aragonite, a metastable form of calcium carbonate that is one and a half times more soluble than calcite (Mucci 1983; Sun et al. 2015). As their shells are susceptible to dissolution, pteropods have been called 'canaries in the coal mine', or sentinel species that signal the impacts of ocean acidification on marine calcifiers (e.g. Bednaršek et al. 2017a, Manno et al. 2017). Although shelled pteropods are already negatively affected in several regions of the global ocean (e.g. Bednaršek et al. 2012b; 2017b; Maas et al. in review), and will likely be seriously threatened if CO_2 levels continue to rise (e.g. Moya et al. 2016; Maas et al. 2016; 2018), little is known about the evolutionary history of the group.

Improving the phylogenetic framework for pteropods and estimating the timing of divergence for major lineages will help determine what effect past periods of high atmospheric CO_2, such as the Paleocene Eocene Thermal Maximum (PETM), have had on their diversification and survivorship. The PETM is widely regarded as the closest geological analogue to the modern rise in ocean-atmosphere CO_2 levels, global warming and ocean acidification (Zachos et al. 2005; Hönisch et al. 2012; Penman et al. 2014). Knowing whether major pteropod lineages have been exposed during their evolutionary history to periods of high CO_2 is important to extrapolate from current experimental and observational studies to predictions of species-level responses to global change over longer timescales.

Pteropods are uniquely suited to shed light on long-term marine evolutionary dynamics, because they are the only living metazoan plankton with a good fossil record (Bé & Gilmer 1977). The only other pelagic groups with abundant fossil records are protists, including foraminifers, radiolarians, coccolithophores, and extinct animal lineages, such as ammonites. The pteropod fossil record extends from a rare internal mold of *Heliconoides* sp. from the Campanian, late Cretaceous (72.1 Million years ago (Ma), Janssen & Goedert 2016) to the present, with abundant fossils from the Eocene onwards (from ~ 56 Ma, reviewed in Janssen & Peijnenburg 2017). However, the fossil record of pteropods is somewhat limited because their shells are very thin and are only preserved in waters above the aragonite saturation depth, which is shallower than the saturation depth of calcite (Gerhardt & Henrich 2001). In addition, several groups of pteropods have only partial shells or are shell-less as adults and thus are rarely preserved in marine sediments. Hence, resolving the evolutionary history of pteropods requires a combination of molecular and fossil-based approaches to resolve past diversification and timing.

While most researchers recognise pteropods as being comprised of two orders, Thecosomata ('sea butterflies') and Gymnosomata ('sea angels'), a recent taxonomic revision (Bouchet et al. 2017) identifies three suborders: 1) Euthecosomata, fully-shelled, omnivorous mucus-web feeders, 2) Pseudothecosomata, a poorly known group with shelled, partially-shelled and unshelled species that also use mucus webs for feeding, and 3) Gymnosomata, with shell-less adults that are specialised predators, primarily on euthecosomes. Progressive evolution towards loss of shells as an adaptation to planktonic life has been proposed for the group (Lalli & Gilmer 1989; Spoel & Dadon 1999), but never fully tested.

Previous attempts to resolve the molecular phylogeny of pteropods have relied on small subsets of genes, and resolution has been limited, especially at deeper nodes, due to large rate heterogeneity and insufficient taxonomic signal (Klussmann-Kolb & Dinapoli 2006; Jennings et al. 2010; Corse et al. 2013; Burridge et al. 2017). Here we used a phylogenomic approach based on transcriptome sequencing to fully resolve the phylogeny of pteropods. Using the pteropod fossil record to calibrate the timing of divergence, we estimate that two major groups of pteropods, 'sea butterflies' and 'sea angels' diverged in the early Cretaceous, and thus must have survived previous global perturbations to the ocean's carbonate system.

Main text (results & discussion)

Robust phylogenomic resolution. We generated new transcriptome data for 22 pteropod samples corresponding to 21 species collected along two basin-scale transects in the Atlantic

Ocean (Table S1 and S2). We also incorporated available data for three additional pteropod species (Moya et al. 2016; Maas et al. 2018; Zapata et al. 2014) and three outgroup species: the sea hare *Aplysia californica*, within the proposed sister group of pteropods (Aplysiida), and two members of Cephalaspidea, *Haminoea antillarum* and *Philine angasi,* from Zapata et al. (2014). Our taxonomic sampling included representatives of all extant families of Euthecosomata, two of three families of Pseudothecosomata, and two of six families of Gymnosomata. All superfamilies of Pteropoda were sampled except Hydromyloidea (Gymnosomata).

We inferred a set of single-copy orthologues using gene family reconstruction from assembled and translated transcripts and selected 2654 single-copy nuclear genes for phylogenetic inference based on their taxonomic representation. These selected genes are well-represented in our transcriptomes with a median of 1815 genes per species, the least being 682 genes (77.4% missing data) for *Diacria trispinosa* (Table S2). We combined these single-copy orthologues in a large data matrix of 834,394 amino acids with 35.75% missing data.

Using the large data matrix (2654 genes) and a site-homogeneous model of evolution ($LG+\Gamma_4$), we recovered a fully resolved phylogenetic tree with maximal support values at all interspecific nodes (Figure 1). To account for the putative limitations of site-homogeneous models that could lead to systematic error, we also applied a site-heterogeneous model (CAT+GTR+Γ) using Bayesian inference (Figure S1). For this analysis, we used a reduced data matrix comprised of the 200 most informative genes (108,008 amino acids, see Methods) and we recovered an identical topology but for a single terminal node (Figure S1).

Pteropod systematics reappraised. Our trees confirm that pteropods are a monophyletic group with sea hares (*Aplysia*) as their closest sister group (Klussmann-Kolb & Dinapoli 2006; Zapata et al. 2014). Pteropods are split into two monophyletic clades: Thecosomata and Gymnosomata, which is congruent with the traditional classification but strongly supported by molecular evidence for the first time. An obvious shared character for pteropods are the wing-like structures or 'parapodia' used for swimming. Histological and ultrastructural studies showed that the muscle arrangements in parapodia are very complex and look similar in Thecosomata and Gymnosomata, supporting a homologous origin (Klussmann-Kolb & Dinapoli 2006). Thecosomata comprise the Euthecosomata and Pseudothecosomata clades, whose member species are all omnivorous mucus-web feeders (Gilmer & Harbison 1986). Their common feeding mechanism is reflected in the well-developed mucus secreting pallial gland that is shared among all thecosomes, as well as a muscular gizzard with which they can

crush the hard exoskeletons of their prey (Lalli & Gilmer 1989). Gymnosomata are shell-less at the adult stage and are specialized carnivorous hunters. They have several morphological characters that set them apart from Thecosomata, including tentacle-like structures called 'buccal cones' and hook sacs to grab and manipulate shelled pteropod prey (Lalli 1970, Klussmann-Kolb & Dinapoli 2006). Hence, the recent revision by Bouchet et al. (2017) with three separate suborders (Euthecosomata, Pseudothecosomata, Gymnosomata) should revert back to the original classification with two main clades: Thecosomata, comprising the Euthecosomata and Pseudothecosomata, and Gymnosomata as shown in Figure 1. Within the fully-shelled Euthecosomata, we obtained maximal support for the coiled (Limacinoidea) and uncoiled (Cavolinioidea) superfamilies as monophyletic sister clades for the first time in a molecular analysis. These results finally stabilize the higher-level taxonomy of the group, which has been debated ever since Cuvier (1804) established the Pteropoda as a separate order of molluscs.

In agreement with previous molecular phylogenetic analyses (Corse et al. 2013; Burridge et al. 2017), we find good support for lower level groupings (e.g. genera *Diacria* and *Limacina*) and recover *Creseis* as the earliest diverging lineage within the uncoiled shelled pteropods. The genus *Clio*, however, is paraphyletic in our analyses with *Clio cuspidata* and *Cuvierina atlantica* grouping together, and *Clio pyramidata* either as a sister taxon to this group (maximum-likelihood tree, Fig. 1) or to the clade *Cavolinia* + *Diacavolinia* + *Diacria* (Bayesian tree, Fig. S1). These results are congruent with the branching obtained using a wider taxon sampling but only three genes (Burridge et al. 2017). Thus, it seems plausible that the genus *Clio* consists of two distinct groups, which could be characterised by distinct larval shell shapes, including *C. cuspidata* and *C. recurva* in one clade, and *C. pyramidata* and *C. convexa* in the other (Janssen 2012). Sampling of additional species for transcriptome sequencing and more detailed morphological analysis are necessary to definitively revise the taxonomy of this genus.

Divergence times of major pteropod lineages. Estimating divergence times based on genome-scale datasets has been shown to be accurate and powerful, however, this depends on the use of realistic evolutionary and clock models as well as a reliable fossil calibration scheme (Tanner et al. 2017; Irisarri et al. 2017). We inferred divergence times of the main pteropod lineages using a recent revision of their fossil record (Janssen & Peijnenburg 2017), which provided eight meaningful calibrations (Fig. 2, Table S3). Within the sister clade of Pteropoda (Aplysiida) the shelled genus *Akera* has by far the best and oldest known fossil record (Cossmann 1895a, 1895b, Valdes & Lozouet 2000) and we chose the oldest confidently identified species of *Akera* (*A. neocomiensis*) to provide the calibration for the

Aplysiida + Pteropoda clade (Table S3). To ensure accurate reconstructions, we chose a realistic model of sequence evolution (CAT-GTR) using the reduced data matrix of 200 genes. We performed cross-validation to select the best clock model (CIR, Figure 2) but also verified that the divergence times reported under alternative clock models, such as autocorrelated log-normal or uncorrelated gamma multipliers, were not markedly different for the major clades (Figure S2, Table S4).

Our phylogenomic time-tree dates the origin of pteropods to the early Cretaceous (139.1 Ma with 95% credibility interval (CrI): 188.2-111.4, Fig. 2), which is substantially older than the estimates based on previous molecular phylogenies (Paleocene and late Cretaceous as estimated by Corse et al. 2013 and Burridge et al. 2017, respectively). While previous estimates were based on a few markers, our analyses are based on a much more comprehensive gene set and rely on more realistic models of evolution and better-curated fossil calibrations. We also find that divergences of the two main lineages, Thecosomata and Gymnosomata, are placed in the Cretaceous period, dated at 129.4 (CrI: 175.8-103.3) and 100.7 (137.0-76.4) Ma, respectively. Of the fully shelled pteropods, all coiled species share a most recent common ancestor at 107 (145.5-85.1) Ma and the uncoiled species at 99.1 (134.7-78.2) Ma.

Different groups of pteropods (sea butterflies and sea angels, species with coiled and uncoiled shells) were already present in the Cretaceous and thus must have survived previous major environmental changes and associated extinctions such as the asteroid impact at the end of the Cretaceous (KT, 66 Ma, Smit & Hertogen 1980; Schulte et al. 2010) and the Paleocene Eocene Thermal Maximum (PETM, 56 Ma, Kennett & Stott 1991; Dickens et al. 1997; Zachos et al. 2005) (Fig. 2). Many pelagic groups disappeared during the well-known mass extinction at the KT boundary (Jablonski 1994), but the multiple environmental factors that changed simultaneously during this period make it difficult to pinpoint a specific cause of these changes, such as ocean acidification (Hönisch et al. 2012). The PETM had an impact on marine calcifiers as shown by a rapid decrease in calcium carbonate content in marine sediments (Luo et al. 2016) and the recording of one of the largest extinctions among deep-sea benthic foraminifers (Kennett & Stott 1991; Schmidt et al. 2018). Planktonic calcifiers were also affected during the PETM, with shifts in species assemblages and changes in species abundance of calcareous nannoplankton, but no clear signal of increased extinction (Gibbs et al. 2006, Bown & Pearson 2009; Kelly et al. 1996; Raffi et al. 2009). For the pteropod fossil record, we see an increase of species from pre-PETM (Thanetian, 2 species) to post-PETM (Ypresian, 32 species) which led to the suggestion that the PETM might have had a triggering effect on pteropod evolution (Janssen et al. 2016).

Evolutionary history of pteropods. Our estimated divergence times for the major pteropod groups predate by far the oldest known fossils for these groups (Fig. 2). The largest discrepancies are found for Gymnosomata and Pseudothecosomata, for which the oldest fossils are from the Chattian (probably a *Clione* sp., 28-23 Ma) and Chattian-Burdigalian periods (*Peracle amberae*, 28-16 Ma), respectively (Janssen 2012). This discrepancy is not surprising as these groups are characterised by reduced shells or no shells at all as adults and their microscopic (larval) shells remain mostly uncharacterised. The pteropod fossil record is generally affected by a strong taphonomic bias as their delicate aragonitic shells preserve poorly. Furthermore, micropaleontologists have traditionally focused on calcitic planktonic calcifiers (coccolithophores, foraminifers) rather than aragonite-producing ones, such as pteropods. This trend is illustrated by plotting the reported diversity of pteropod species through time (Figure 2), showing a sharp increase in the number of recent species (162) compared to previous periods (21 species for the Pleistocene and a median of 34.5 species for the preceding Neogene periods). Since pteropods are considered to be promising new proxy carriers in palaeoceanography, recording surface ocean temperature and carbonate ion concentrations (Wall-Palmer et al. 2012; Keul et al. 2017), this renewed interest will hopefully result in a reappraisal of their fossil record in the coming years.

Surprisingly, we find similar Cretaceous origins for the coiled (Limacinoidea) and uncoiled (Cavolinioidea) shelled pteropods even though the fossil record for coiled shells extends much further (Campanian, late Cretaceous) than for uncoiled shells (Ypresian, early Eocene). The species with straight, bilaterally symmetrical shells were thought thought to have derived from coiled ancestors (*Altaspiratella*) that show a trend of despiralisation in the fossil record starting during the early Ypresian and giving rise to the oldest representatives of Cavolinioidea (*Camptoceratops* and *Euchilotheca*) (first suggested by Boas (1886) and reviewed in Janssen & Peijnenburg 2017). It is interesting to note that shell microstructure differs fundamentally between coiled and uncoiled pteropods. Uncoiled species have an outer prismatic layer and a thick inner layer with a unique helical microstructure (Bé et al. 1972; Li et al. 2015), whereas coiled shells have simple prismatic and crossed lamellar microstructures (Lalli & Gilmer 1989), similar to the outgroup *Aplysia* (Marin et al. 2018). Examination of shell microstructures of fossil species could shed further light on the phylogenetic placement of the fossils. For instance, the fossil *Camptoceratops priscum* from the early Eocene was found to have helical microstructure similar to extant Cavolinioidea (Curry & Rampal 1979). A recent report by Garvie et al. (in review) of potentially much older uncoiled pteropod-like fossils from Mesozoic and Paleocene rocks of the southern United States found that their microstructure is, in contrast, crossed-lamellar. If future analyses show that these are indeed

pteropods, despiralisation must have occurred multiple times throughout their evolutionary history. Reports of Cretaceous pteropods remain extremely rare despite considerable paleontological effort, which suggests that pteropods were not abundant and/or very poorly preserved during this period. Notably, Cretaceous deposits are often dominated by limestones, which are unsuitable for the preservation of thin-walled aragonitic pteropod shells (Janssen & Peijnenburg 2017).

We found that the shelled groups (sea butterflies) diverged before the unshelled ones (sea angels), suggesting that unshelled species evolved from shelled ancestors (Fig. 2). However, we do not see a clear trend toward gradual loss of shells in our phylogeny. This could be further assessed by sampling more species belonging to the elusive Pseudothecosomata, with species ranging from fully-shelled (*Peracle* spp.) to partially-shelled (*Cymbulia*, *Corolla*, *Gleba* spp.) and even entirely unshelled as adults (*Desmopterus* spp.). In our phylogeny, we only included one *Peracle* species possessing an external coiled calcareous shell and one *Cymbulia* species bearing a gelatinous 'pseudoconch'. Since the pteropod outgroups are benthic gastropods (Aplysiida, Cephalaspidea) with mostly coiled or reduced shells, the ancestor of pteropods most likely lived on the seafloor and had a coiled shell (Klussmann-Kolb & Dinapoli 2006; Corse et al. 2013). Some authors proposed that pteropods evolved in a neotenic fashion, where larvae of benthic gastropods became sexually mature and lived their full life cycle in the open water column, because of 'juvenile' shell characters such as the sinistral spiral and aragonitic shell structure (Lemche 1948; Huber 1993). However, this hypothesis has been questioned by Jägersten (1972), who argued that the foot – an adult feature – played a decisive role in the transition from a benthic to a holoplanktonic existence by transforming from a creeping organ to swimming fins. It is interesting to note that a similar hypothesis was proposed for the only other extant group of holoplanktonic gastropods, the heteropods (Pterotrachoidea). For this group, the earliest fossil, *Coelodiscus minutus*, dates back to the early Jurassic and represents the oldest known holoplanktonic gastropod (Teichert & Nützel 2015). Colonization of the open water column required numerous adaptations in both groups of holoplanktonic gastropods independently: pteropods belonging to Heterobranchia and heteropods belonging to Caenogastropoda.

Fate of sea butterflies and angels from Cretaceous to Anthropocene. Pteropods evolved in the early Cretaceous and thus were contemporaries of other major calcifying groups in the open ocean, such as ammonites and foraminifers (Fig. 2). Based on their fossil records, Tajika et al. (2018) suggested that planktonic gastropods filled the ecological niche left empty by juvenile ammonites after their extinction at the end of the Cretaceous. However, this seems less likely given our earlier estimated origins of both sea butterflies (thecosomes) and sea

295 angels (gymnosomes). Instead, we propose that sea angels evolved as specialized predators of
296 sea butterflies during the Cretaceous, perhaps in an evolutionary arms race (Seibel et al. 2007)
297 in which thecosomes evolved stronger and ever more sophisticated shells (e.g. *Diacria*,
298 *Cavolinia*) and gymnosomes evolved adaptations for prey capture and extraction, specific to
299 the shell shapes of their prey. For instance, *Clione* feed exclusively on certain *Limacina*
300 species by manipulating the coiled shells with their flexible buccal cones and extracting the
301 prey with their hooks, whilst *Pneumodermopsis* feed on long and straight-shelled *Creseis*
302 species using their long and flexible proboscis for prey extraction. There are also accounts of
303 unsuccessful attacks, which happen when sea butterflies retract rapidly enough and far
304 enough into their shell (Conover & Lalli 1972, Lalli & Gilmer 1989). Moreover, even though
305 thecosomes are eaten by a variety of predators ranging from planktonic crustaceans to fish,
306 whales and seabirds, no other pelagic group than gymnosomes feeds predominantly on
307 thecosomes. Hence, we consider it plausible that different groups of pteropods co-evolved
308 during a period that is referred to as the Marine Mesozoic Revolution. In this major
309 evolutionary episode, a series of ecological shifts took place on the sea floor because of the
310 evolution of powerful, relatively small, shell-destroying predators, including a massive
311 radiation of predatory gastropods in the Early Cretaceous (Vermeij 1977; Harper 2003). This
312 forced benthic gastropods to develop heavily armoured shells and perhaps also to escape into
313 the open water column, as was suggested for earlier geological periods (Signor & Vermeij
314 1994, Teichert & Nützel 2015). Furthermore, during the mid-late Cretaceous major changes
315 in ocean circulation, stratification and nutrient partitioning took place which were favorable
316 for plankton evolution, in particular for planktonic calcifiers (Leckie et al. 2002).
317
318 Although the open ocean may have been a refuge for gastropods in the early Cretaceous, it is
319 an increasingly challenging habitat to survive in during the Anthropocene. Planktonic
320 gastropods have evolved thin, fragile shells of aragonite that are sensitive to ocean
321 acidification, and most species live in surface waters where CO_2 is absorbed by the ocean.
322 Incubation experiments with shelled pteropods mimicking future ocean conditions have
323 shown that elevated pCO_2 and undersaturated aragonite conditions cause decreased
324 calcification rates (Comeau et al. 2012), shell dissolution (Lischka et al. 2011), increased
325 mortality (Bednaršek et al. 2017b; Thabet et al. 2015) and differential expression of genes
326 involved in neurofunction, ion transport, and shell formation (Moya et al. 2016; Maas et al.
327 2018). However, such experiments have primarily assessed phenotypic responses in short-
328 term, single-generation studies, and thus cannot take into account the abilities of organisms to
329 acclimate or adapt to changing conditions over longer timescales. The geological record,
330 alternatively, can provide insight into long-term evidence of ocean acidification and the
331 associated responses of marine calcifiers. However, the fossil record of pteropods appears far

from complete and hence, we need to rely on estimates of molecular divergence times to resolve the tempo and pattern of their evolution. The fact that pteropods have survived previous episodes of ocean acidification, such as during the PETM, does not, however, mean that they are infinitely resilient to current changes. Current rates of carbon release from anthropogenic sources are at least an order of magnitude higher than we have seen for the past 66 million years (Zeebe et al. 2016). Although our results suggest resilience of pteropods to past ocean acidification, it is unlikely that they have ever, during their entire evolutionary history, experienced global change of the magnitude and speed that we see today.

Acknowledgements

We appreciate the comments of J. Paps, D. Gavriouchkina and M. Malinsky on earlier versions of this manuscript. We acknowledge the Oxford Genomics Centre, Wellcome Trust Centre for Human Genetics, for performing the transcriptome sequencing. We would like to thank A.K. Burridge for collecting samples and T. Smythe, G. Tarran, and A. Rees for cruise leadership and support for participation in the AMT programme. This study contributes to the international IMBeR project and is contribution number 339 of the AMT programme.

Funding

This research and KTCAP were supported by a Vidi grant 016.161351 from the Netherlands Organisation for Scientific Research (NWO), a Tera van Benthem Jutting grant from the Amsterdam University Fund and a KNAW ecology fund UPS/297/Eco/1403J. DWP received funding from the European Union's Horizon 2020 research and innovation programme under the Marie Sklodowska-Curie grant agreement No 746186 (POSEIDoN). EG was supported by National Science Foundation (USA) grants OCE-1338959 and OCE-1255697. FM was supported by internal funding of the Okinawa Institute of Science and Technology to the Molecular Genetics Unit. The Atlantic Meridional Transect is funded by the UK Natural Environment Research Council through its National Capability Long-term Single Centre Science Programme, Climate Linked Atlantic Sector Science (grant number NE/R015953/1).

Author contributions

KTCAP conceived this study and obtained funding. KTCAP and EG collected and identified specimens at sea. KTCAP and FM carried out the labwork. FM led the data analyses. KTCAP and AWJ reviewed the fossil record and provided calibrations. KTCAP and FM drafted the manuscript, and all others commented.

Methods

Sample collection. Pteropod specimens were collected on Atlantic Meridional Transect (AMT) cruises 22 and 24 (2012, 2014), using 0.71m diameter bongo and RMT1 nets towed obliquely between a median of 305 m depth and the sea surface (200, 333 µm nets; Table S1). Animals were sorted and identified live from bulk plankton, preserved in RNALater (Invitrogen) and flash frozen in liquid nitrogen, with storage at -80°C.

Transcriptome sequencing and filtering. RNA was extracted using RNAeasy micro or mini kits (Qiagen) after homogenisation with a Tissuelyser (Qiagen). The number of individuals used for extraction varied from 1, in most cases, to 10 (Table S1). RNA quantity was determined by fluorimetry using a Qubit (Invitrogen) and RNA integrity was assessed using the Xperion system (Biorad). RNA-seq libraries were prepared using the TruSeq RNA Library preparation kit (Illumina) and between 12 and 33M paired-end reads per sample were sequenced for 100 cycles on a HiSeq2000 platform at the Wellcome Trust Centre for Human Genetics (Oxford). 2.3 to 6.6 Gb of DNA sequence data were obtained from each of 22 samples, ensuring accurate *de novo* transcriptome assemblies (Table S2). Reads were deposited to the SRA under the bioproject accession XXXX. After quality assessment with Fastqc (Andrews 2010), reads were trimmed using sickle (Joshi 2011) and subsequently assembled using *Trinity* (v2.3.2) with default parameters and a k-mer of 25 (Grabherr et al. 2011).

To avoid cross-contamination between samples sequenced on the same Illumina lanes (possibly due to index 'hopping'), we applied a filtering procedure based on relative transcript expression across datasets, similar to the one implemented in Croco (Simion et al. 2018). Briefly, for the assembled transcriptome of each dataset, we measured expression level using Kallisto (v0.42.4) (Bray et al. 2016) in each of the multiple datasets sequenced simultaneously. We calculated the ratio of TPMs between the putatively contaminating datasets and the original dataset, and excluded transcripts with a contaminant enrichment greater than two-fold enrichment, and a minimal count lower than 2 in the original dataset. Across datasets, a median 6% of transcripts were excluded on the first criterion and a median 26% on the second.

De novo assembled transcriptomes usually include a high degree of redundancy, as alternative transcripts derived from the same genes are distinguished in the assembly. As this might constitute a problem for orthology assignment, we clustered transcripts based on the fraction

of remapped reads that they share. To do so, we mapped reads from transcriptomes back to transcripts using Bowtie2 enabling up to 50 multi-mappers (-k 50) and processed the resulting alignments with Corset (v1.06) (Davidson and Oshlack 2014). Then, we estimated transcript expression using Kallisto (v0.43.1) (Bray et al. 2016) and we selected the most highly expressed transcript with each Corset cluster as a reference transcript for subsequent steps. The best open reading frame (ORF) for each of these selected transcripts was predicted using Trans-decoder (v5.0.2) using a blast against a version of swissprot limited to metazoan taxa (e-value 10^{-5}) (Haas et al. 2008).

Phylogenetic analyses. We conducted orthology inference using the OMA package (v2.3.0), which performs smith-waterman alignment and identifies orthologues based on evolutionary distance (Roth et al. 2008). We selected single-copy orthologues (OMA groups) represented by at least one of the three outgroup taxa (*Aplysia californica*, *Haminoea antillarum* or *Philine angasi*) and at least half of the 28 ingroup taxa. These cut-offs yielded 2654 single-copy orthologues suitable for phylogenetic analysis. For each orthologue family, protein sequences were aligned using Mafft and poorly aligned regions trimmed using Trimal (Capella-Gutiérrez et al. 2009) for sites with a gap in more than 75% of taxa (-gt 0.15) and applying a low minimum similarity threshold (-st 0.001). The concatenation of these 2654 orthologuous genes yields a supermatrix of 834,394 positions with a total fraction of 35.75% missing data. We performed Maximum-likelihood reconstruction with ExaML (v3.0.17) using a partitioned site-homogeneous model (one partition per orthologue) and a LG+Γ_4 model (Kozlov et al. 2015). Node support was calculated using 100 bootstrap replicates inferred with independently generated starting trees (Figure 1). To compare results with a site-heterogeneous model, we used Bayesian inference and a reduced dataset (because the complete dataset would be computationally intractable). We selected a subset of 200 genes which showed the maximal average bootstrap support when analysed independently (using RAxML v8.1.18, LG+Γ_4 model and 100 rapid bootstraps) (Stamatakis 2014). The concatenation of these 200 genes generated a 108,008 amino acid alignment. This alignment was analysed using Phylobayes-MPI (v1.6) assuming a CAT+GTR+Γ_4 model) with chains run for more than 1500 generations with 500 discarded as burnin. Chain convergence was checked and maxdiff found at 0 (Rodrigue & Lartillot 2014).

Molecular divergence time inference. We used Phylobayes (v4.1c) to infer molecular divergence times using the reduced 200 gene supermatrix and the topology from Figure 1 (ML analysis) (Lartillot et al. 2009). We used the CAT+GTR+Γ_4 model of sequence evolution and we assayed several clock models, the lognormal autocorrelated process (-ln), the CIR process and the uncorrelated gamma multiplier process, with a birth-death prior on

443 divergence time, and soft bounds on calibration points (Lepage et al. 2007). We applied 9
444 calibration points with uniform priors based on the fossil records of pteropods (Table S3) and
445 a root prior of 150 Myr with a standard deviation of 70 Myr. Using a 10-fold cross validation
446 procedure, we found a best fit of the CIR process over log-normal and uncorrelated gamma
447 processes (Figure 2 and Figure S2). The root prior was conservatively chosen based on the
448 oldest known heterobranch (e.g. *Cylindrullina* dated 240 Ma, (Ponder & Lindberg 2008)) and
449 *Akera* fossils (*Akera mediojurensis* and *Akera neocomiensis* dated at 163-166 Ma and 133
450 Ma, respectively, Cossmann 1895a;b; Cossmann 1896). Broad deviations were used to
451 account for the uncertainty of the fossil record. The consistency of the root prior was assessed
452 by running chains without the data, which yielded a root age of 154 ± 32 Myr.
453
454 Data availability
455
456 Alignments and files generated during analyses including Bayesian sample and bootstrap
457 replicates are available at the following address: XXXX.
458
459 References
460
461 Andrews, S. 2010. FastQC: A Quality Control Tool for High Throughput Sequence Data.
462 Babraham Bioinformatics, Babraham Institute, Cambridge, United Kingdom.
463
464 Bé, A.W.H., MacClintock, C. & Currie, D.C., 1972. Helical shell structure and growth of the
465 pteropod *Cuvierina columnella* (Rang) (Mollusca, Gastropoda). *Biomineralization Res. Reps.*
466 4:47-79.
467
468 Bé, A.W.H., Gilmer, R.W., 1977. A zoogeographic and taxonomic review of
469 euthecosomatous Pteropoda. In: Ramsay, A.T.S. (Ed.), Oceanic Micropalaeontology.
470 Academic Press, London, pp. 733–808.
471
472 Bednaršek, N. et al. 2012a. The global distribution of pteropods and their contribution to
473 carbonate and carbon biomass in the modern ocean. *Earth System Science Data* 4, 167–186.
474
475 Bednaršek, N. et al. 2012b. Extensive dissolution of live pteropods in the Southern Ocean.
476 *Nat. Geosci.* **5,** 881–885.
477
478 Bednaršek, N. et al. 2017a. New ocean, new needs: application of pteropod shell dissolution
479 as a biological indicator for marine resource management. *Ecol. Indicators* 76, 240-244.

Bednaršek, N. et al. 2017b. Exposure history determines pteropod vulnerability to ocean acidification along the US West Coast. *Nat. Commun.*, **7,** 1–12 (2017).

Berner, R.A. & Honjo, S. 1981. Pelagic sedimentation of aragonite - its geochemical significance. *Science* 211: 940-942.

Boas, J.E.V. 1886a. Spolia Atlantica. Bidrag til Peropodernes. Morfologi og systematik samt til Kundskaben om deres geografiske udbredelse. *K. danske Vidensk. Selsk. Skr.* 4: 1-231.

Bouchet, P. et al. 2017. Revised classification, nomenclator and typification of gastropod and monoplacophoran families. *Malacologia* 61: 1-526.

BouDagher-Fadel, M.K., 2015. Biostratigraphic and geological significance of planktonic foraminifera. UCL Press, University College London.

Bown, P. & Pearson, P. 2009. Calcareous plankton evolution and the Paleocene/Eocene Thermal Maximum event: New evidence from Tanzania, *Mar. Micropaleontol* 71:60–70.

Bray, N.L., Pimentel, H., Melsted, P. & Pachter, L. 2016. Near-Optimal Probabilistic RNA-Seq Quantification. *Nature Biotechnology* 34 (5): 525–27.

Buitenhuis, E. T., Le Quéré, C., Bednaršek, N. & Schiebel, R. 2019. Large contribution of pteropods to shallow $CaCO_3$ export. *Glob. Biogeochem. Cycles* 33: 458- 468.

Burridge, A.K. et al. 2017. Time-calibrated molecular phylogeny of pteropods. *PlosONE* 12(6): e0177325.

Capella-Gutiérrez, S., Silla-Martínez, J.M. & Gabaldón, T. 2009. TrimAl: A Tool for Automated Alignment Trimming in Large-Scale Phylogenetic Analyses. *Bioinformatics* 25 (15): 1972–73.

Comeau, S., Gattuso, J.-P., Nisumaa, A.-M. & Orr, J. 2012. Impact of aragonite saturation state changes on migratory pteropods. *P. Roy. Soc. B-Biol. Sci.* **279,** 732–738.

Conover, R.J. & Lalli, C.M. 1972. Feeding and growth in *Clione limacina* (Phipps), a pteropod mollusc. *J. expl mar. Biol. Ecol.* 9:279-302.

Corse, E. et al. 2013. Phylogenetic analysis of Thecosomata Blainville, 1824 (Holoplanktonic Opisthobranchia) using morphological and molecular data. *PLoS ONE* 8(4):e59439.

Cossmann, M. 1895a. Essais de paléoconchologie comparée. Première livraison. Comptoir Geologique, Paris.

Cossmann, M. 1895b. Contribution à la paléontologie française des terrains jurassiques. Études sur les gasteropodes des terrains jurassiques. Mémoires de la Société Géologique de France. *Paléontologie* 14:1-165p

Curry, D. & Rampal, J. 1979. Shell microstructure in fossil thecosome pteropods. *Malacologia* 18:23-25.

Cuvier, G., 1804. Mémoire concernant l'animal de l'*Hyale*, un nouveau genre de mollusques nus, intermédiaire entre l'*Hyale* et la *Clio* et l'établissement d'un nouvel ordre dans la clase des mollusques. *Annls Mus. Hist. nat. Paris* 4: 223-34.

Davidson, N.M. & Oshlack, A. 2014. Corset: Enabling Differential Gene Expression Analysis for de Novo Assembled Transcriptomes. *Genome Biology* 15 (7): 410.

Dickens, G., Castillo, M.M. & Walker, J.C.G., 1997. A blast of gas in the latest Paleocene: simulating first-order effects of massive dissociation of oceanic methane hydrate. *Geology* 25:259-262.

Garvie, C.L., Goedert, J.L. & Janssen, A .W. (in review). Paleogene and Late Cretaceous Pteropoda (Mollusca, Gastropoda, Heterobranchia) from North America. *Zootaxa*.

Gerhardt, S. & Henrich, R., 2001. Shell preservation of *Limacina inflata* (Pteropoda) in surface sediments from the Central and South Atlantic Ocean: a new proxy to determine the aragonite saturation state of water masses. *Deep-Sea Res. I* 48: 2051–2071.

Gibbs, S.J. et al. 2006. Nannoplankton extinction and origination across the Paleocene-Eocene Thermal Maximum. *Science* 314:1770-1773.

552 Gilmer, R.W. & Harbison, G.R. 1986. Morphology and field behaviour of pteropod molluscs:
553 feeding methods in the families Cavoliniidae, Limacinidae and Peraclididae (Gastropoda:
554 Thecosomata). *Mar. Biol.* 91: 47-57.
555
556 Grabherr, M.G. et al. 2011. Full-Length Transcriptome Assembly from RNA-Seq Data
557 without a Reference Genome. *Nature Biotechnology* 29 (7): 644–52.
558
559 Haas, B.J. et al. 2008. Automated Eukaryotic Gene Structure Annotation Using
560 EVidenceModeler and the Program to Assemble Spliced Alignments. *Genome Biology* 9 (1):
561 R7.
562
563 Harper, E.M. 2003. The Mesozoic marine revolution. Pp. 433-445 in: Patricia H. Kelley,
564 Michał Kowalewski and Thor A. Hansen (eds). Predator-prey interactions in the fossil record.
565 Topics in Geobiology, Vol. 20. New York, Kluwer.
566
567 Hönisch, B., et al. 2012. The geological record of ocean acidification. *Science* 335: 1058-
568 1063.
569
570 Huber, G. 1993. On the cerebral nervous system of marine heterobranchia (Gastropoda). *J*
571 *Molluscan Stud.* 59:381-420.
572
573 Hunt, B.P.V. et al. 2008. Pteropods in Southern Ocean ecosystems. *Prog. Oceanogr.* 78, 193-
574 221.
575
576 Irisarri, I. et al. 2017. Phylotranscriptomic consolidation of the jawed vertebrate timetree.
577 Nature Ecology and Evolution 1:1370-1378.
578
579 Jablonski, D. 1994. Extinctions in the fossil record. *Phil. Trans. Roy. Soc. B* 344:11-17.
580
581 Jägersten, G. 1972. Evolution of the Metazoan life cycle. New York, Academic Press. 282 pp.
582
583 Janssen, A.W. 2012. Late Quaternary to Recent holoplanktonic Mollusca (Gastropoda) from
584 bottom samples of the eastern Mediterranean Sea: systematics, morphology. *Bollettino*
585 *Malacologico* 48:1–105.
586

587 Janssen, A.W. & Goedert, J.L. 2016. Notes on the systematics, morphology and
588 biostratigraphy of fossil holoplanktonic Mollusca, 24. First observation of a genuinely Late
589 Mesozoic thecosomatous pteropod. *Basteria* 80, 59-63.
590
591 Janssen, A.W., Sessa, J.. & Thomas, E., 2016. Pteropoda (Mollusca, Gastropoda,
592 Thecosomata) from the Paleocene-Eocene Thermal Maximum (United States Atlantic Coastal
593 Plain). *Palaeontologia Electronica,* 19.3.47A: 1-26.
594
595 Janssen, A.W. & Peijnenburg, K.T.C.A. 2017. An overview of the fossil record of Pteropoda
596 (Mollusca, Gastropoda, Heterobranchia). *Cainozoic Research* 17: 3-10.
597
598 Jennings, R.M., Bucklin, A., Ossenbrügger H. & Hopcroft R.R. 2010. Species diversity of
599 planktonic gastropods (Pteropoda and Heteropoda) from six ocean regions based on DNA
600 barcode analysis. *Deep-Sea Res II* 57: 2199–2010.
601
602 Joshi, N.A, & Fass, J.N. 2011. Sickle: A Sliding-Window, Adaptive, Quality-Based
603 Trimming Tool for FastQ Files. 2011. https://github.com/najoshi/sickle.
604
605 Kelly, D. C. et al. 1996. Rapid diversification of planktonic foraminifera in the tropical
606 Pacific (ODP Site 865) during the Late Paleocene Thermal Maximum, *Geology* 24: 423–426.
607
608 Kennett, J.P. & Stott, L.D. 1991. Abrupt deep-sea warming, palaeoceanographic changes and
609 benthic extinctions at the end of the Paleocene. *Nature* 353: 225-229.
610
611 Keul, N. et al. 2017. Pteropods are excellent recorders of surface temperature and carbonate
612 ion concentration. *Scientific Reports* 7: 12645.
613
614 Klussmann-Kolb, A. & Dinapoli, A. 2006. Systematic position of the pelagic Thecosomata
615 and Gymnosomata within Opisthobranchia (Mollusca, Gastropoda) – revival of the
616 Pteropoda. *Journal of Zoological Systematics and Evolutionary Research* 44(2):118–129.
617
618 Kozlov, A.M., Aberer, A.J. & Stamatakis, A. 2015. ExaML Version 3: A Tool for
619 Phylogenomic Analyses on Supercomputers. *Bioinformatics* 31 (15): 2577–79.
620
621 Lalli, C.M. 1970. Structure and function of the buccal apparatus of *Clione limacina* (Phipps)
622 with a review of feeding in gymnosomatous pteropods. *J. expl mar. Biol. Ecol.* 4:101-118.
623

624 Lalli, C.M. & Gilmer, R.W. 1989. Pelagic Snails: The Biology of Holoplanktonic Gastropod
625 Molluscs. Stanford University Press, California.
626
627 Lartillot, N., Lepage, T. & Blanquart, S. 2009. PhyloBayes 3: A Bayesian Software Package
628 for Phylogenetic Reconstruction and Molecular Dating. *Bioinformatics* 25 (17): 2286–88.
629
630 Leckie, R.M., Bralower, T.J. & Cashman, R. 2002. Oceanic anoxic events and plankton
631 evolution: biotic response to tectonic forcing during the Cretaceous. *Paleaceanography* 17:1-
632 29.
633
634 Lemche, H. 1948. Northern and Arctic tectibranch gastropods. I/II. K. danske Vidensk. Selsk.
635 Skr. 5:1-136.
636
637 Lepage, T., Bryant, D., Philippe, H. & Lartillot, N. 2007. A General Comparison of Relaxed
638 Molecular Clock Models. *Molecular Biology and Evolution* 24 (12): 2669–80.
639
640 Li, L., Weaver, J.C. & Ortiz, C. 2015. Hierarchical structural design for fracture resistance in
641 the shell of the pteropod *Clio pyramidata*. *Nature Communications* 6:6216.
642
643 Lischka, S., Büdenbender, J., Boxhammer, T. & Riebesell, U. 2011. Impact of ocean
644 acidification and elevated temperatures on early juveniles of the polar shelled pteropod
645 *Limacina helicina*: mortality, shell degradation, and shell growth. *Biogeosciences* 8: 919–932.
646
647 Luo, Y. et al. 2016. An alternative model for $CaCO_3$ over-shooting during the PETM:
648 biological carbonate compensation. *Earth and Planetary Science Letters* 453:223-233.
649
650 Maas, A.E., Lawson, G.L. & Wang, Z.A. 2016. The metabolic response of thecosome
651 pteropods from the North Atlantic and North Pacific Oceans to high CO_2 and low O_2.
652 *Biogeosci. Discuss.* 1–43.
653
654 Maas, A.E., Lawson, G.L., Bergan, A.J. & Tarrant, A.M. 2018. Exposure to CO_2 influences
655 metabolism, calcification and gene expression of the thecosome pteropod *Limacina*
656 *retroversa*. *Journal of Experimental Biology* 221:1-13.
657

658 Maas, A. E., Lawson, G. L., Bergan, A. J., Wang, Z. A. & Tarrant, A. M. in review. Seasonal
659 variation in physiology and shell condition of the pteropod *Limacina retroversa* in the Gulf of
660 Maine relative to life cycle and carbonate chemistry. *Progress in Oceanography.*
661
662 Manno, C. et al. 2017. Shelled pteropods in peril: assessing vulnerability in a high CO_2 ocean.
663 *Earth-Science Rev.* 169: 132–145.
664
665 Manno, C. et al. 2018. Threatened species drive the strength of the carbonate pump in the
666 northern Scotia Sea. *Nature Communications* 9:4592.
667
668 Marin, F. et al. 2018. Skeletal organic matrices in molluscs: origin, evolution, diagenesis.
669 *Biomineralization* 325-332.
670
671 Moya, A. et al. 2016. Near-future pH conditions severely impact calcification, metabolism
672 and the nervous system in the pteropod *Heliconoides inflatus*. *Glob. Change Biol.* 22, 3888–
673 3900.
674
675 Mucci, A. 1983. The solubility of calcite and aragonite in seawater at various salinities,
676 temperatures, and one atmosphere total pressure. *Am J Sci* 283:780–799
677
678 Peters, S.E., Kelly, D.C. & Fraass, A.J. 2013. Oceanographic controls on the diversity and
679 extinction of planktonic foraminifera. *Nature* 493: 398-401.
680
681 Penman, D.E. et al. 2014. Rapid and sustained surface ocean acidification during the
682 Paleocene-Eocene Thermal Maximum. *Paleoceanography* 29:357-369.
683
684 Ponder, W. & Lindberg, D.R. 2008. Phylogeny and Evolution of the Mollusca. University of
685 California Press.
686
687 Raffi, I., Backman, J., Zachos, J.C. & Sluijs, A. 2009. The response of calcareous nannofossil
688 assemblages to the Paleocene Eocene Thermal Maximum at the Walvis Ridge in the South
689 Atlantic. *Mar. Micropaleontol.* 70: 201–212.
690
691 Rodrigue, N. & Lartillot, N. 2014. Site-Heterogeneous Mutation-Selection Models within the
692 PhyloBayes-MPI Package. *Bioinformatics* 30 (7): 1020–21.
693

694 Roth, A.C.J., Gonnet, G.H. & Dessimoz, C. 2008. Algorithm of OMA for Large-Scale
695 Orthology Inference. *BMC Bioinformatics* 9 (1): 1.
696
697 Schmidt, D.N. et al. 2018. Strategies in times of crisis - insights into the benthic foraminiferal
698 record of the Palaeocene-Eocene Thermal Maximum. *Philosophical Transactions of the*
699 *Royal Society A* 376:20170328.
700
701 Schulte, P., et al. 2010. The Chicxulub asteroid impact and mass extinction at the Cretaceous-
702 Paleogene boundary. *Science* 307: 1214-1218.
703
704 Signor, P.W. & Vermeij, G.J. 1994. The plankton and the benthod: origins and early history
705 of an evolving relationship. *Paleobiology* 20:297-319.
706
707 Simion, P. et al. 2018. A Software Tool 'CroCo' Detects Pervasive Cross-Species
708 Contamination in next Generation Sequencing Data. *BMC Biology* 16 (1): 28.
709
710 Smit, J. & J. Hertogen, 1980. An extraterrestrial event at the Cretaceous-Tertiary boundary.
711 *Nature* 285:198-200.
712
713 Stamatakis, A. 2014. RAxML Version 8: A Tool for Phylogenetic Analysis and Post-Analysis
714 of Large Phylogenies. *Bioinformatics* 30 (9): 1312–13.
715
716 Sun, W. et al. 2015. Nucleation of metastable aragonite CaCO3 in seawater. Proceedings of
717 the National Academy of Sciences 112: 3199-3204.
718
719 Tajika, A., Nützel A. & Klug C. 2018. The old and the new plankton: ecological replacement
720 of associations of mollusc plankton and giant filter feeders after the Cretaceous? *PeerJ*
721 6:e4219; DOI 10.7717/peerj.4219
722
723 Tanner, A.R. et al. 2017. Molecular clocks indicate turnover and diversification of modern
724 coleoid cephalods during the Mesozoic Marine Revolution. *Proceedings of the Royal Society*
725 *B* 284:20162818.
726
727 Teichert, S. & Nützel A. 2015. Early Jurassic anoxia triggered the evolution of the oldest
728 holoplanktonic gastropod *Coelodiscus minutus* by means of heterochrony. *Acta*
729 *Palaeontologica Polonica* 60: 269-276.
730

731 Thabet, A. A., Maas, A.E., Lawson, G.L. & Tarrant, A.M.. 2015. Life cycle and early
732 development of the thecosomatous pteropod *Limacina retroversa* in the Gulf of Maine,
733 including the effect of elevated CO_2 levels. *Marine Biology* 162: 2235-2249.
734
735 Valdes, A. & Lozouet, P. 2000. Opisthobranch molluscs from the Tertiary of the Aquitaine
736 Basin (South-Western France), with descriptions of seven new species and a new genus.
737 *Palaeontology* 43:457-479.
738
739 Van der Spoel, S. & Dadon, J.R. 1999. Pteropoda. In: Boltovskoy D. (Ed.), South Atlantic
740 Zooplankton. Backhuys Publishers, Leiden, pp. 649-706.
741
742 Vermeij, G. 1977. The Mesozoic marine revolution: evidence from snails, predators and
743 grazers. *Paleobiology* 3:245-258.
744
745 Wall-Palmer, D. et al. 2012. Pteropods from the Caribbean Sea: variations in calcification as
746 an indicator of past ocean carbonate saturation. *Biogeosciences* 9, 309-315.
747
748 Yacobucci, M.M. 2015. Macroevolution and paleobiogeography of Jurassic-Cretaceous
749 ammonoids. Pp. 189-228 in: C. Klug, D. Korn, K. De Baets, I. Kruta, and R.H. Mapes (eds.).
750 Ammonoid Paleobiology: from Macroevolution to Paleogeography. Topics in Geobiology,
751 Vol. 44. Dordrecht, Springer.
752
753 Zachos, J.C. et al. 2005. Rapid acidification of the ocean during the Paleocene-Eocene
754 Thermal Maximum. *Science* 308: 1611-1615.
755
756 Zapata, F. et al. 2014. Phylogenomic analyses of deep gastropod relationships reject
757 Orthogastropoda. *Proceedings of the Royal Society B* 281:20141739.
758
759 Zeebe, R.E., Ridgwell, A. & Zachos, J.C. 2016. Anthropogenic carbon release rate
760 unprecedented during the past 66 million years. *Nature Geoscience* 9:325-329.

Figures

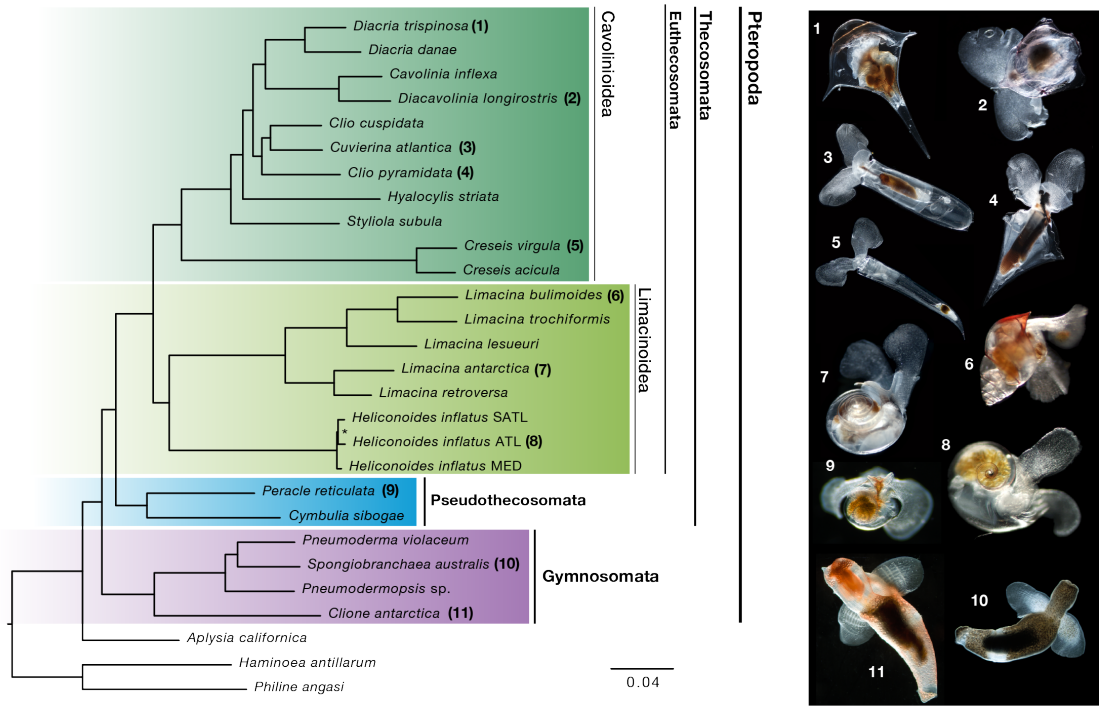

Figure 1. **Phylogenomics resolves evolutionary relationships of pteropods**. Euthecosomes (fully shelled species) and pseudothecosomes (ranging from fully shelled to unshelled species) are recovered as sister clades for the first time in a molecular analysis restoring the Thecosomata ('sea butterflies') as a natural group. Thecosomata and Gymnosomata ('sea angels') are monophyletic sister clades congruent with traditional morphology-based views. The superfamilies Cavolinioidea with uncoiled shells and Limacinoidea with coiled shells are also recovered as monophyletic sister clades.

Maximum Likelihood phylogeny of 25 pteropod taxa, plus 3 outgroups assuming a LG+Γ model. The dataset comprises 2654 genes, concatenated as 834,394 amino acid positions with 35.8% missing data. A nearly identical topology is obtained modelled under CAT-GTR+Γ with a reduced dataset of 200 genes (Figure S1). Higher taxonomic divisions are indicated. All nodes receive maximal bootstrap support, except the node with an asterisk (bootstrap 95%). On the right are images of living pteropod species (numbers correspond with taxon labels, not to scale) collected and photographed by the authors. Scale bar indicates substitutions per site.

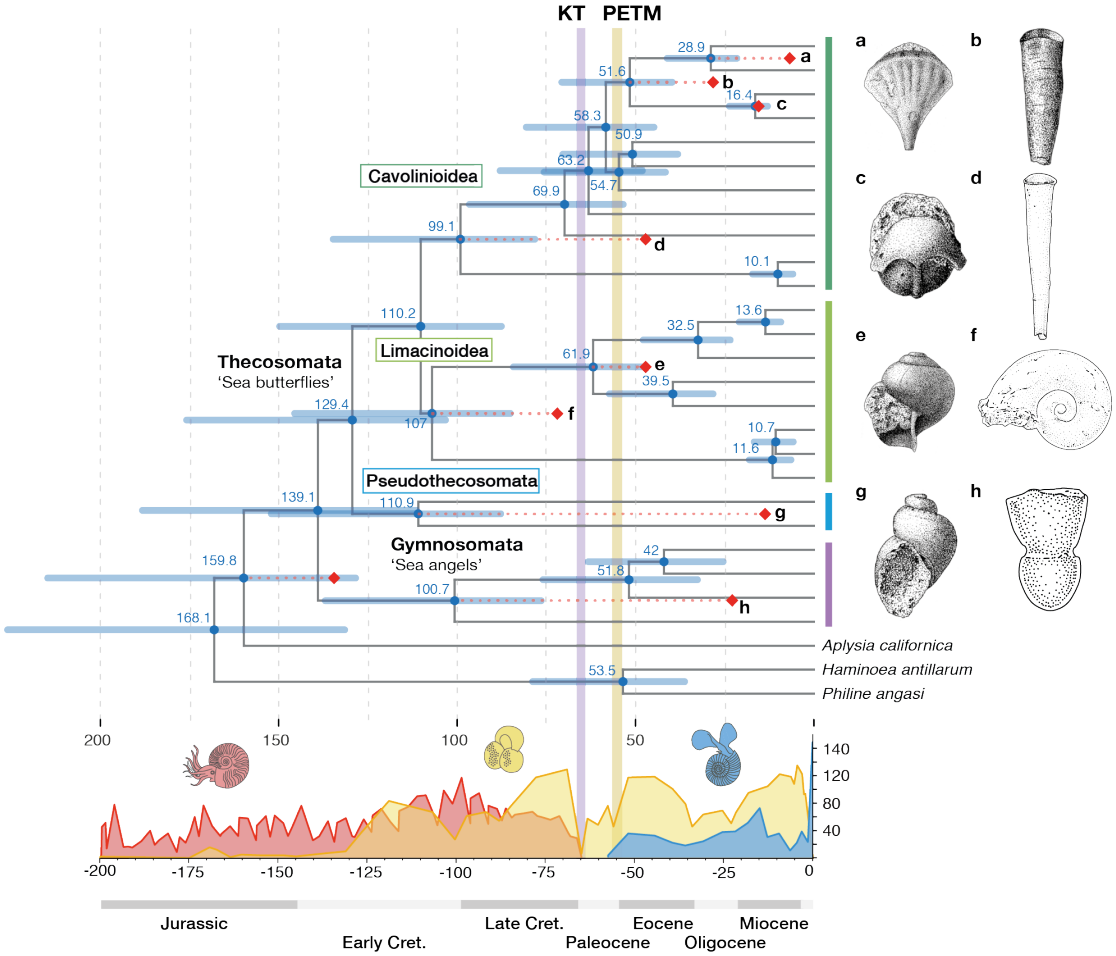

Figure 2. **All major lineages of pteropods diverged in the Cretaceous and thus must have survived previous major global change events.** Chronogram of pteropods (25 taxa and 3 outgroups) based on 200 genes, concatenated as 108,008 amino acid positions, analysed under a CAT-GTR+Γ evolutionary model and CIR relaxed clock model. Red diamonds indicate fossil-calibrated nodes (see Table S3) with red dotted lines to show divergence from minimum ages of the fossils. Two major global change events are indicated as KT (Cretaceous-Tertiary asteroid impact, 66 Ma) and PETM (Paleocene Eocene Thermal Maximum, ~56 Ma). Curves for ammonite (red), planktonic foraminifer (yellow), and pteropod (blue) species diversity through time are based on sediment records from Yacobucci (2015), Boudagher-Fadel (2015), and our own data base (available from the authors on request), respectively.

Drawings of fossil species used for calibrations correspond to nodes a: *Diacria sangiorgii* (7.2 Ma), b: *Vaginella gaasensis* (28.1 Ma), c: *Cavolinia microbesitas* (16 Ma), d: *Euchilotheca ganensis* (47.8 Ma), e: *Limacina gormani* (47.8 Ma), f: *Heliconoides sp.* (72.1 Ma), g: *Peracle amberae* (16 Ma), and h: *Clione ? imdinaensis* (23 Ma). The oldest outgroup calibration is *Akera neocomiensis* (133 Ma, no drawing available).

Supplementary Figures

Figure S1. **Phylogenomics resolves evolutionary relationships of pteropods**. Euthecosomes (fully shelled species, green) and pseudothecosomes (ranging from fully shelled to unshelled species, blue) are recovered as sister clades for the first time in a molecular analysis restoring the Thecosomata ('sea butterflies') as a natural group. Thecosomata and Gymnosomata ('sea angels', purple) are monophyletic sister clades congruent with traditional morphology-based views. The superfamilies Cavolinioidea with uncoiled shells and Limacinoidea with coiled shells are also recovered as monophyletic sister clades.

Bayesian phylogeny of 25 pteropod taxa, plus 3 outgroups assuming a CAT+GTR+Γ_4 model using Phylobayes-MPI. The dataset was comprised of 200 selected genes (see Methods), concatenated as 108,008 amino acid positions. All nodes received maximal posterior probabilies.

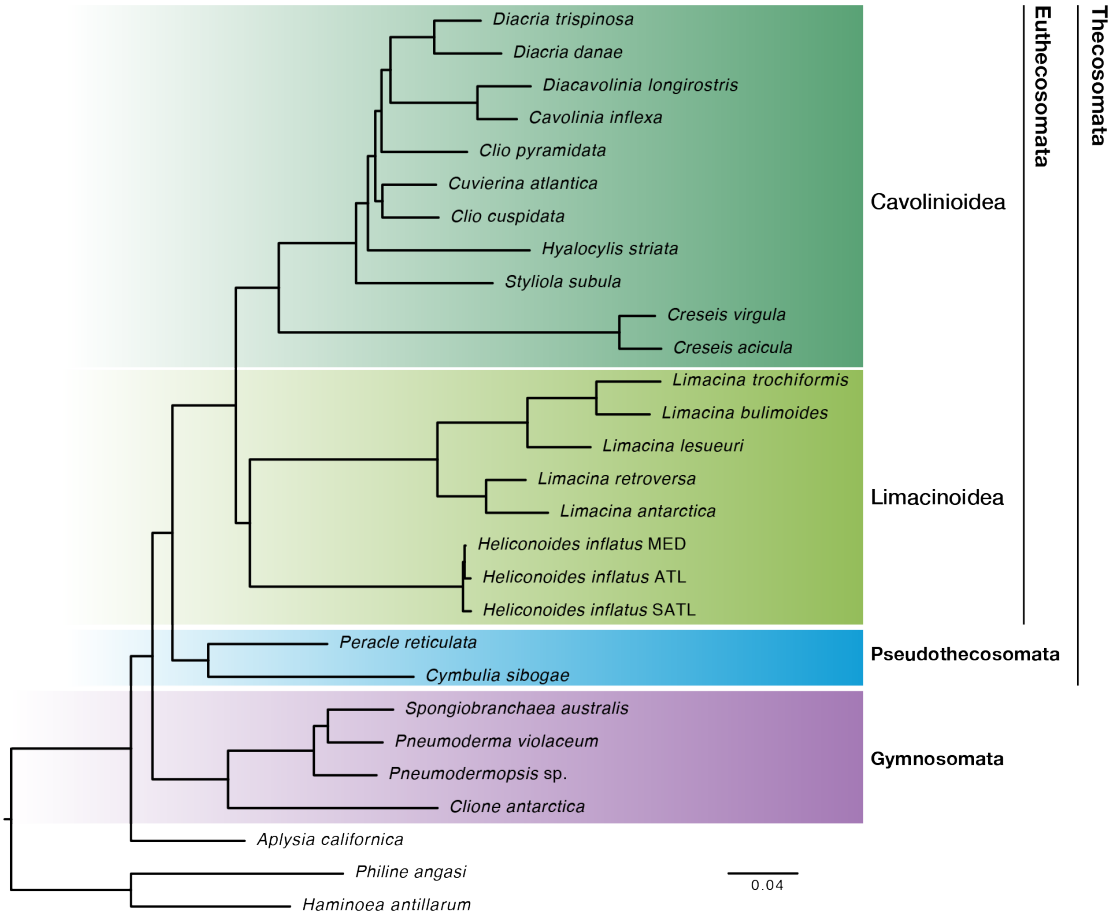

Figure S2. **Divergence times for major pteropod clades under different clock models were not markedly different.** Bayesian phylogenies to infer molecular divergence times using the reduced 200 genes supermatrix, the topology of Figure 1 and a CAT+GTR+Γ_4 model of sequence evolution (see Methods) with three different clock models: the CIR process (CIR, see also Figure 2), the lognormal autocorrelated process (Log-normal), and the uncorrelated gamma multiplier process (UGAM).

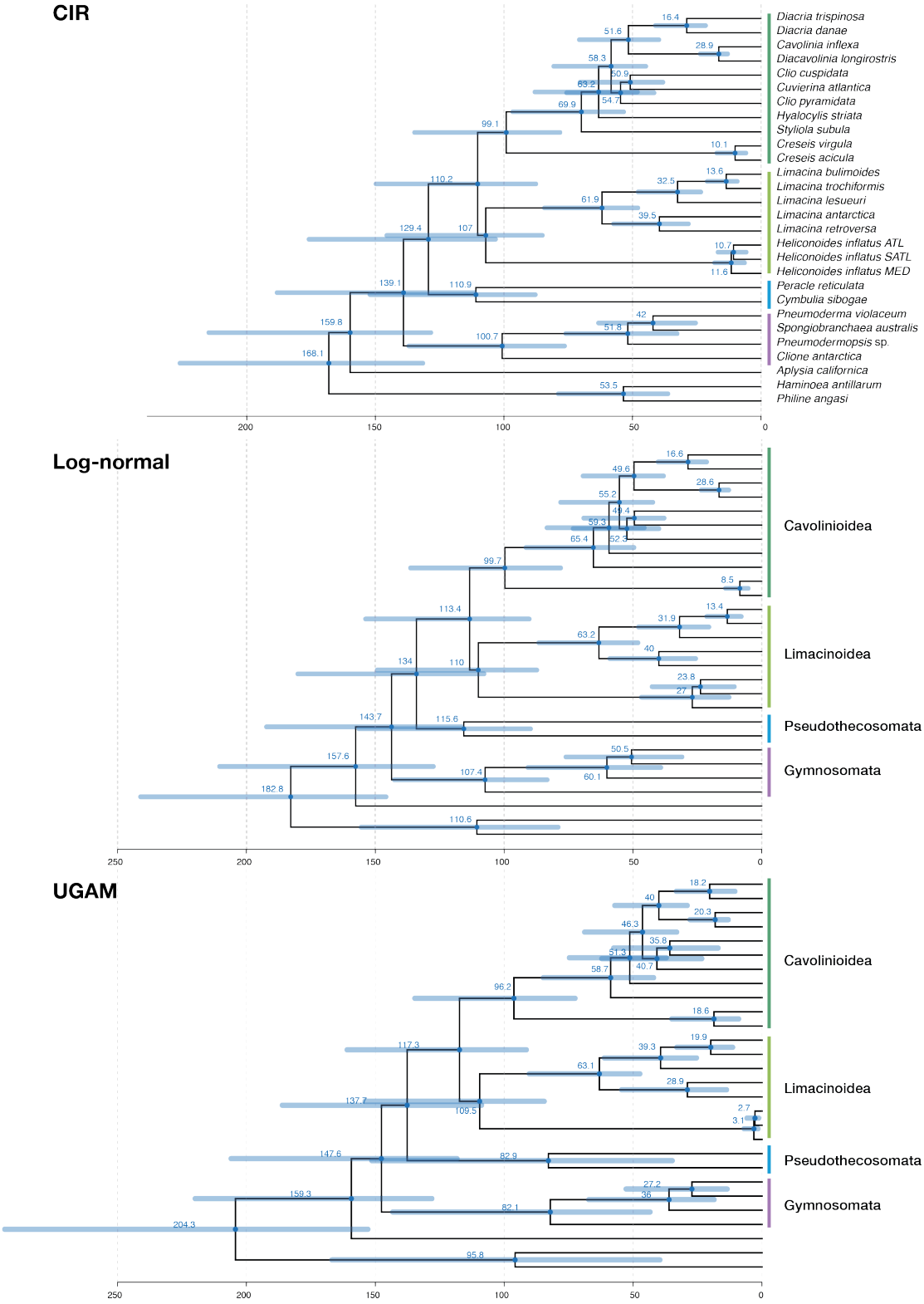

Supplementary tables

Table S1. Sampling details of pteropod taxa for which new transcriptome data were collected.

Species	Taxonomic group	Latitude	Longitude	Collection date	Max depth of sample (m)	Net type, mesh size	number of individuals used in RNAextraction
Cavolinia inflexa	Euthecosomata	30° 35.9 S	25° 48.3 W	22/10/14	163	Bongo, 200µm	2
Clio cuspidata	Euthecosomata	39° 24.6 N	22° 28.6 W	01/10/14	274	Bongo, 200µm	1
Clio pyramidata	Euthecosomata	18° 19.9 N	28° 48.5 W	07/10/14	91	Bongo, 200µm	1
Creseis acicula	Euthecosomata	20° 51.3 S	25° 04.7 W	20/10/14	309	Bongo, 200µm	3
Creseis virgula	Euthecosomata	18° 19.9 N	28° 48.5 W	07/10/14	91	Bongo, 200µm	3
Cuvierina atlantica	Euthecosomata	28° 21.7 S	25° 27.3 W	11/11/12	301	Bongo, 333µm	1
Cymbulia sibogae	Pseudothecosomata	11° 22.2 N	27° 19.9 W	09/10/14	70	Bongo, 200µm	1
Diacavolinia longirostris	Euthecosomata	6° 37.1 N	28° 19.0 W	29/10/12	404	Bongo, 333µm	1
Diacria danae	Euthecosomata	24° 27.4 S	25° 02.5 W	21/10/14	323	Bongo, 200µm	2
Diacria trispinosa	Euthecosomata	24° 03.4 N	29° 54.5 W	06/10/14	258	Bongo, 200µm	1
Heliconoides inflatus (ATL)	Euthecosomata	4° 03.0 N	26° 27.8 W	30/10/12	388	Bongo, 333µm	10
Heliconoides inflatus (S ATL)	Euthecosomata	37° 53.6 S	28° 44.2 W	25/10/14	372	Bongo, 200µm	6
Hyalocylis striata	Euthecosomata	7° 17.1 N	26° 29.5 W	11/10/14	329	Bongo, 200µm	1
Limacina antarctica	Euthecosomata	44° 37.4 S	40° 41.5 W	29/10/14	350	Bongo, 200µm	5
Limacina bulimoides	Euthecosomata	24° 27.4 S	25° 02.5 W	21/10/14	323	Bongo, 200µm	5
Limacina lesueuri	Euthecosomata	14° 12.4 N	27° 55.7 W	09/10/14	305	Bongo, 200µm	4
Limacina trochiformis	Euthecosomata	25° 29.1 S	25° 00.0 W	09/11/12	153	RMT1, 333µm	1
Peracle reticulata	Pseudothecosomata	14° 12.4 N	27° 55.7 W	09/10/14	305	Bongo, 200µm	3
Pneumoderma violaceum	Gymnosomata	10° 46.8 N	27° 12.4 W	10/10/14	323	Bongo, 200µm	1
Pneumodermopsis sp.	Gymnosomata	31° 20.4 S	26° 06.0 W	23/10/14	330	Bongo, 200µm	1
Spongiobranchaea australis	Gymnosomata	41° 28.6 S	33° 51.5 W	27/10/14	228	Bongo, 200µm	1
Styliola subula	Euthecosomata	30° 35.9 S	25° 48.311 W	22/10/14	163	Bongo, 200µm	2

Table S2. Details of 28 transcriptome datasets used in phylogenomic analyses. N_reads is the number of sequenced paired-end reads, N_pept is the number of predicted peptides among transcripts. N_OG is the number of selected single-copy orthologues recovered for this species. P_miss_OG is the percentage of missing single-copy orthologues for the taxon, P_gaps is the fraction of gaps and P_miss_tot is the total fraction of missing data in the alignment for the taxon (gaps and missing genes).

Species	Order	Taxonomic group	accession	N_reads	N_pept	N_OG	P_miss_OG	P_gaps	P_miss_tot
Aplysia californica	Aplysiida	Outgroup	ftp.broadinstitute	-	92469	2616	1.09	1.6	2.69
Cavolinia inflexa	Pteropoda	Euthecosomata	SRRXXXXX	14107853	20521	1729	35.51	2.17	37.68
Clio cuspidata	Pteropoda	Euthecosomata	SRRXXXXX	15473224	21307	1222	56	1.05	57.05
Clio pyramidata	Pteropoda	Euthecosomata	SRRXXXXX	15596539	24705	1665	39.3	2.12	41.42
Clione antarctica	Pteropoda	Gymnosomata	SRR1505107	20282761	19813	1915	29.53	2.62	32.16
Pneumodermopsis sp.	Pteropoda	Gymnosomata	SRRXXXXX	18094803	18984	1396	51.35	1.24	52.59
Creseis acicula	Pteropoda	Euthecosomata	SRRXXXXX	12027779	27003	1806	33.19	2.82	36.01
Creseis virgula	Pteropoda	Euthecosomata	SRRXXXXX	14105581	26726	1824	34.12	3.06	37.18
Cuvierina atlantica	Pteropoda	Euthecosomata	SRRXXXXX	28558114	20994	1966	28.34	2.99	31.33
Cymbulia sibogae	Pteropoda	Pseudothecosomata	SRRXXXXX	13430464	14494	1166	57.8	1.83	59.63
Diacavolinia longirostris	Pteropoda	Euthecosomata	SRRXXXXX	14469630	21220	1582	44.76	2.22	46.98
Diacria danae	Pteropoda	Euthecosomata	SRRXXXXX	25218341	36533	1673	38.09	1.23	39.32
Diacria trispinosa	Pteropoda	Euthecosomata	SRRXXXXX	13123731	16800	682	76.48	0.87	77.36
Haminoea antillarum	Cephalaspidea	Outgroup	SRR1505111	-	39489	1821	35.68	5.68	41.36
Heliconoides inflatus (ATL)	Pteropoda	Euthecosomata	SRRXXXXX	33421222	20283	1109	66.97	2.08	69.05
Heliconoides inflatus (S ATL)	Pteropoda	Euthecosomata	SRRXXXXX	18330623	33123	1925	29.03	2.73	31.76
Heliconoides inflatus (MED)	Pteropoda	Euthecosomata	PRJNA312154	-	25016	2434	7.83	2.2	10.03
Hyalocylis striata	Pteropoda	Euthecosomata	SRRXXXXX	20300621	33352	2360	10.42	2.23	12.65
Limacina bulimoides	Pteropoda	Euthecosomata	SRRXXXXX	18046287	28764	1799	34.54	2.81	37.35
Limacina antarctica	Pteropoda	Euthecosomata	SRRXXXXX	19486196	28954	2221	15.92	2.07	17.99
Limacina lesueuri	Pteropoda	Euthecosomata	SRRXXXXX	14648179	24430	1793	33.53	2.1	35.64
Limacina retroversa	Pteropoda	Euthecosomata	PRJNA260534	-	40077	2376	10.62	2.53	13.15
Limacina trochiformis	Pteropoda	Euthecosomata	SRRXXXXX	14412701	35829	2004	25.99	2.75	28.74
Peracle reticulata	Pteropoda	Pseudothecosomata	SRRXXXXX	17876973	27998	1776	35.18	2.43	37.61
Philine angasi	Cephalaspidea	Outgroup	SRR1505129	11881480	33219	2037	23.05	5.81	28.87

Pneumoderma violaceum	Pteropoda	Gymnosomata	SRRXXXXX	16362957	24989	2148	17.78	2.21	19.99
Spongiobranchaea australis	Pteropoda	Gymnosomata	SRRXXXXX	18191206	20998	1621	40.7	1.66	42.36
Styliola subula	Pteropoda	Euthecosomata	SRRXXXXX	16115592	29755	2062	20.76	2.33	23.09

Table S3. Nine fossil calibrations used in the molecular clock analyses. Letters refer to nodes labelled a-i in the chronogram of Figure 2.

Calibrated node	Fossil species	Epoch: stage	Minimum age (Ma)	Reference
a: *Diacria*	*Diacria sangiorgii*	Miocene: Tortonian	7.2	Scarsella 1934
b: *Cavolinia*+*Diacavolinia*+*Diacria*	*Vaginella gaasensis*	Oligocene: Rupelian	28.1	Cahuzac & Janssen 2010
c: *Cavolinia*+*Diacavolinia*	*Cavolinia microbesitas*	Miocene: Late Burdigalian	16	Janssen 2012
d: Cavolinioidea	*Euchilotheca ganensis*	Eocene: Yresian	47.8	Curry 1982
e: *Limacina*	*Limacina gormani*	Eocene: Ypresian	47.8	Cahuzac & Janssen 2010
f: Limacinoidea	*Heliconoides* sp.	Cretaceous: Campanian	72.1	Janssen & Goedert 2016
g: Pseudothecosomata	*Peracle amberae*	Oligocene: Chattian-Burdigalian	16	Janssen 2012
h: Gymnosomata	*Clione ? imdinaensis*	Oligocene: Chattian	23	Janssen 2012
i: Pteropoda+*Aplysia*	*Akera neocomiensis*	Cretaceous: Early Hauterivian	133	Cossmann 1895a, b

References (supl. material)

Cahuzac, B. & A. W. Janssen, 2010. Eocene to Miocene pteropods (Gastropoda, Euthecosomata) from the Aquitaine Basin, SW France. Scripta Geologica, 141: 1-193

Cossmann M. 1895a. Essais de paléoconchologie comparée. Première livraison. Comptoir Geologique, Paris.

Cossmann, M. 1895b. Contribution à la paléontologie française des terrains jurassiques. Études sur les gasteropodes des terrains jurassiques. Mémoires de la Société Géologique de France. Paléontologie 14:1-165p

Curry, D., 1982. Ptéropodes éocènes de la tuilerie de Gan (Pyrénées-Atlantiques) et de quelques autres localités du SW de la France. Cahiers de Micropaléontologie, 4: 35-44, 1 pl.

Janssen, A. W., 2012. Systematics and biostratigraphy of holoplanktonic Mollusca from the Oligo-Miocene of the Maltese Archipelago. Bollettino del Museo Regionale di Scienze Naturali, Torino, 28(2)(2010): 197-601.

Janssen, A. W. & J. L. Goedert. 2016. Notes on the systematics, morphology and biostratigraphy of fossil holoplanktonic Mollusca, 24. First observation of a genuinely Late Mesozoic tecosomatous pteropod. Basteria 80 (1-3):59-63.

Scarsella, F., 1934. Di una nuova specie di pteropodo del Miocene appenninico. Bollettino della. Società Geologica Italiana, 53(2): 177-181. pl. 13.